THE STRONG INFLUENCE OF VIEWING GEOMETRY AND SURFACE TEXTURE ON THE REFLECTANCE SPECTRA OF SMALL BODIES AND METEORITES

S. Potin[1], P. Beck[1], B. Schmitt[1].
[1]Université Grenoble Alpes, CNRS, Institut de Planétologie et d'Astrophysique de Grenoble (IPAG), 414 rue de la Piscine 38400 Saint-Martin d'Hères, France. (sandra.potin@univ-grenoble-alpes.fr)

Introduction: Reflectance spectroscopy is commonly used to analyse the composition of distant airless bodies. The spectral slope and absorption features, if detected, are characteristics of the mineralogy and structure of the surface. Several asteroids classifications are based on the shape of the reflectance spectra in the visible and near-infrared spectral range [1, 2].

It is established that the reflectance of a surface depends on the geometry under which it is measured. The first example being the photometric phase curves, presenting the general albedo as a function to the phase angle [3].

We propose to analyse the dependency of all the spectral characteristics (photometry, slope and absorption bands) with the observation geometry using bidirectional reflectance spectroscopy measurements.

Samples: Meteorites are the best accessible analogues of the Solar System small bodies. Their reflectance spectra match those of their parent bodies, and each of the different types represents a specific class of asteroids [4]. We chose several meteorites samples of different petrologies and alteration histories. All samples were manually ground but not sieved to keep a wide distribution of grain sizes. A few samples were large enough to perform a first bidirectional reflectance distribution function (BRDF) measurement on the intact rock. We also analysed a highly porous agglomerate of Ceres simulant resulting from a sublimation experiment [5].

Measurements: We used the home-made spectro-gonio radiometer SHADOWS [6] to analyse the chosen surfaces under 70 different geometrical configurations (incidence, emergence, azimuth angles). Spectra are acquired from 340 nm to 4200 nm every 20 nm, with a spectral resolution varying from 4.2 nm to 30 nm.

The measured reflectance is determined relative to measurements of calibrated Spectralon and Infragold reflectance targets.

Results: For each sample, we analyse the effect of the measurement geometry on all the characteristics of the reflectance spectra.

Photometry. The variation of photometry with the geometry is investigated through the BRDF. The BRDFs are plotted using a polar representation, where the angular position of the dot corresponds to the observation geometry of the measurement (at fixed incidence), and its distance from the center represents the measured value of the reflectance (see Fig. 1). Using this representation, the BRDF of a perfectly lambertian surface will appear as a semi-circle.

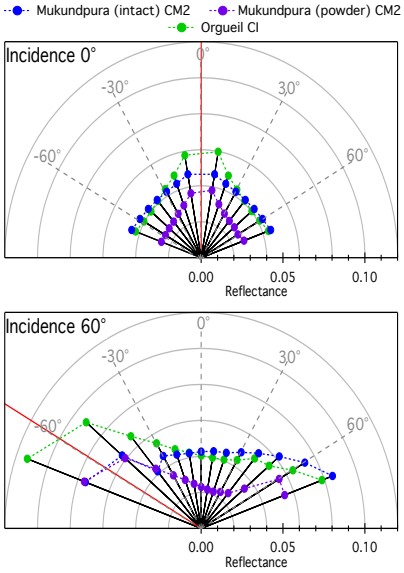

Figure 1: BRDF at 560 nm (out of any absorption feature) of an intact chip of Mukundpura compared to powdered samples of Mukundpura and Orgueil. Top panel: incidence 0°, Bottom panel: incidence 60°.

Figure 1 shows that the BRDF of a surface depends mostly on the texture of the surface, not its mineralogical composition. Two powders will present similar BRDFs behaviours with a strong backscattering, independently of its general albedo, but will differ from an intact bloc displaying a stronger forward scattering behaviour.

Spectral slope and reddening. The spectral slope is calculated as the ratio between the reflectance measured at two separated wavelengths outside of possible absorption features:

$$Slope = {}^{R^{500\,nm}}/_{R^{2000\,nm}}$$

A spectral slope greater than 1 suggests a rather red sample, while a slope smaller than 1 indicates a blue spectrum (see Fig. 2).

The spectral reddening represents the evolution of the slope with the geometry. It is calculated as the ratio between the slopes at a given phase angle g and at the smallest phase angle available (10° in our measurements).

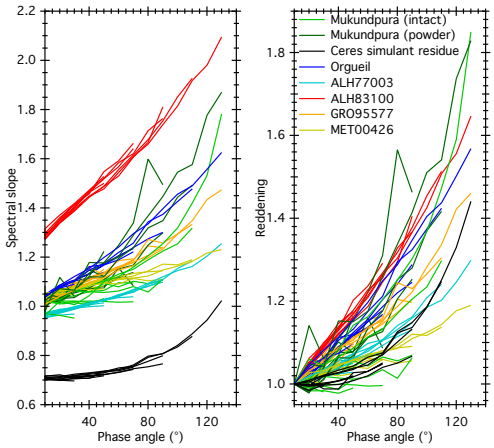

Figure 2: Spectral slope and reddening with increasing phase angle of meteorites samples and the porous sublimation residue.

In case of asteroids observation, a red slope is often linked to an irradiated surface. However, at wide phase angle, the observation geometry effect on the spectral slope can become as strong as the reddening by irradiation. When comparing textures, we found that powdered samples are typically redder than the intact chips [7].

Absorption features. The depth of the absorption bands is also geometry dependent. For each feature strong enough to be detected, the band depth is calculated as:

$$BD = 1 - {R^{band}}/{R^{continuum}}$$

with R^{band} the reflectance of the sample at the center of the absorption feature, and $R^{continuum}$ the calculated reflectance of the continuum at the same wavelength. We considered a linear continuum between the two inflexion points of the band.

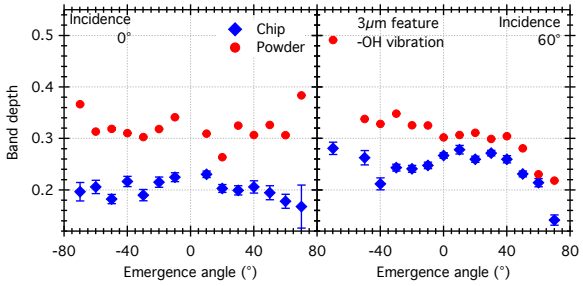

Figure 3: Band depth of the 3μm feature at incidence 0° (left panel) and 60° (right panel). Blue: intact chip, Red: powdered sample. Figure from [7].

We found that the powdered samples tend to present deeper absorption features than the intact chips. With increasing phase angle, all spectral features become fainter, until complete disappearance in some cases [7]. This can be explained by the increasing number of photons directly scattered out of the sample without entering any of the grains.

Conclusion: The bidirectional reflectance spectroscopy of a surface shows important variations with the observation geometry of the measurements. All characteristics of the spectra are impacted: the photometry changes according to the incidence and emergence angles, and with increasing phase angle, the measured spectra tend to become redder with shallower absorption features. The observation geometry strongly affects the shape of surface reflectance spectra and so has to be taken into account in the analysis of in situ or ground-based spectroscopy measurements.

Aknowledgments: The authors would like to thank F. Moynier for the sample of the Mukundpura meteorite, and S. Schröder for his authorization to include the BRDF of the sublimation residue in the analysis.

References: [1] Bus S.J. and Binzel R.P. (2002) *Icarus, 158*, 146-177. [2] DeMeo F.E. et al. (2009) *Icarus, 202*, 160-180. [3] Lane A.P. and Irvine W.M. (1973) *APJ, 78*, 267-277. [4] Vernazza P. and Beck P. (2015) *Planetesimals, chap.16*, 269-297. [5] Poch O. et al. (2014) *Icarus, 267,* 154-173 [6] Potin S. et al. (2018) *Applied Optics, 57*, 8279–8296. [7] Potin S. et al. (2019) *Icarus, 333*, 415-428.